

Comparison of a discrete-cell and continuum model of two-dimensional ventricular tissues under modulation of Cx43

Shengzhe Li¹, Danya Agha-Jaffar¹, Dimitrios Panagopoulos¹, Konstantinos Ntagiantas², Ariana J F Hawkins¹, Liliang Wang³, Prapa Kanagaratnam¹, Rasheda A Chowdhury^{1,#}, Chris D Cantwell^{4,#}

¹ National Heart and Lung Institute, Imperial College London, London, United Kingdom

² Department of Bioengineering, Imperial College London, London, United Kingdom

³ Department of Mechanical Engineering, Imperial College London, London, United Kingdom

⁴ Department of Aeronautics, Imperial College London, London, United Kingdom

These authors contributed equally

Abstract

Cardiac arrhythmias such as atrial fibrillation (AF), ventricular fibrillation (VF) and ventricular tachycardia (VT) are growing causes of morbidity and mortality across the world. To aid the discovery of the mechanisms driving these arrhythmias, in-silico models have been developed to simulate signal propagation in cardiac tissues.

Continuum models such as monodomain and bidomain approaches are the most common methods to represent multicellular electrical activity. These approaches have been successfully applied on the whole heart and large-scale tissues with acceptable approximation. However, they may not be appropriate for microscopic scale simulations. It is known that cellular remodelling, including the development of scars, changes in ion channels or gap junctions play a role in arrhythmogenesis. However, in patients and laboratory models, where these occur simultaneously, the direct effect and importance of single factors are difficult to determine.

Discrete-cell models represent action potential generation and propagation in individual cells and provide a more accurate cell-level simulation, but at much greater computational cost.

In this study, 2D simulations of ventricular tissues with a range of gap junction distributions, informed by biological staining experiments, are performed. Both continuum and discrete-cell models are applied to the same tissues and their propagation patterns are compared. While the continuum model accurately captures propagation with uniform Cx43 distribution, the discrete-cell model provides better accuracy with heterogeneous distributions.

1. Introduction

Cardiac arrhythmia incidence rates are progressively increasing [1]. Some arrhythmias such as ventricular tachycardia or fibrillation (VT or VF) are life-threatening within just a few seconds [2]. Myocardial infarct, heart failure and some valve diseases can lead to VT/ VF. Abnormalities in the gap junctions, which connect individual myocytes, and the presence of scar in the ventricles are associated with VT and VF as they can lead to abnormal electrical pathways [3].

Numerous two- and three-dimensional numerical in-silico cardiac models have been created to investigate the electrical activation of the human left ventricle to further understand the mechanism of VT/ VF [4]. These models include two parts: the ion channels model (action potential (AP) changes of one cell) and the propagation model (transmission through the tissue)[5].

Propagation models can be continuum models or discrete models. Continuum models can be beneficial when simulating electrical propagation within a large area, even the whole heart, as the simulated domain is homogenised, giving a macroscopic representation of AP propagation in short simulation times. However, some pathological changes at the microscopic level, such as abnormal gap junctions, can not be accurately captured. Conversely, the discrete-cell model incorporates the details of the AP propagation between every cell [6]. Therefore, discrete-cell models can theoretically provide more accurate results than continuum models by allowing for the inclusion of cell-level detail such as localised gap junction abnormalities, albeit with additional computational time costs.

This in-silico study focuses on characterising the influence of continuum and discrete models on two-dimensional simulations of human left ventricular tissue, with biologically informed gap junctional abnormalities.

2. Methodology

A $1.2 \text{ mm} \times 1.2 \text{ mm}$ square of human left ventricular myocardium monolayer is created using virtual cardiac monolayers (VCT) [7] for simulation with the discrete propagation model. VCT allows virtual cells to be seeded on fibers, leading to similar anisotropy to that observed in vivo. The virtual monolayer is shown in Figure 1. The size of the monolayer is selected based on a previous study carried out by Dias et al [8]. In that study, the biological cell monolayers were seeded on a micro electrode array plate (MEA) consisting of 60 electrodes (diameter $30 \mu\text{m}$ with $200 \mu\text{m}$ inter-electrode distance). We model this biological preparation size with the central 6×6 electrodes in each direction leading to an effective measurement area of $1 \text{ mm} \times 1 \text{ mm}$. To simulate dimensions similar to the MEA, the size of the simulation domains should be only slightly larger than the electrode area, to minimise unnecessary computational cost. Therefore, a $1.2 \text{ mm} \times 1.2 \text{ mm}$ 2D square domain is generated. Another comparable domain is created using Gmsh [9] for use with the continuum propagation model.

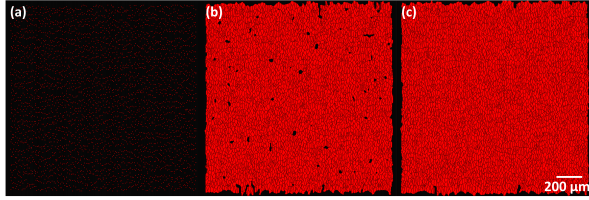


Figure 1. (a) Cells seeded in a $1.2 \text{ mm} \times 1.2 \text{ mm}$ domain. (b) Cells in the "growing" process. (c) Final grown monolayer.

A $0.2 \text{ mm} \times 0.2 \text{ mm}$ area with abnormal gap junctions is introduced into the lower left corner of both domains by reducing conductivity in line with biological experiments carried by Peters et al. [10]. To be more specific, the conductivities are set to 4 mS/mm in the healthy area and 20 mS/mm in the area with abnormal gap junctions for both the continuum model and the discrete-cell model.

A total of 36 locations are selected on each simulation domain, corresponding to the electrode locations of the MEA plate, and simulated electrograms (EGMs) were obtained from the simulations using both the continuum model and the discrete-cell model. The simulation domains are shown in Figure 2.

The action potential propagation simulations were carried out using the CardiacEPSolver built on Nektar++, a high-order spectral/hp element framework [11, 12]. The Ten Tusscher human LV ion-channel model and in-house propagation models (both continuum model and discrete-cell model) were used [6, 13]. The resting potential was set to -81 mV , the monolayers were stimulated from the right

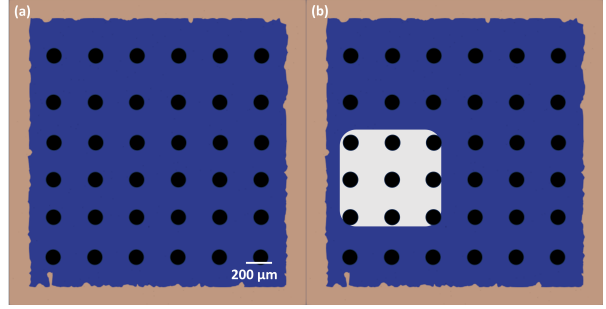


Figure 2. (a) A healthy $1.2 \text{ mm} \times 1.2 \text{ mm}$ monolayer with electrodes. (b) Monolayer with an abnormal gap junction area, 9 electrodes are located in the abnormal area, the conductivity of the gap junctions within the abnormal area was set to $1/5$ of it from the normal area.

edge, creating a wavefront from right to left [14]. To compare the outputs of the discrete cell model and continuum model, simulated action potential propagation and unipolar electrograms (EGMs) were generated and compared. For EGM analysis, 11 time domain features were calculated using an in-house feature extraction code written in Python 3.9. Some important features are shown in Figure 3.

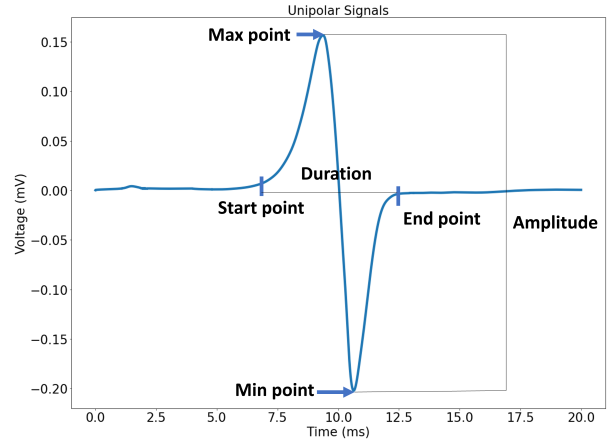


Figure 3. Examples of some of the calculated unipolar EGM features used to compare the electrograms generated by continuum and discrete-cell models.

3. Results

The simulations of the AP propagation are shown in Figure 4 where the influence of the area with abnormal gap junctions on the propagation is clearly visible.

The simulation time using the discrete cell model of the healthy monolayer take 19.5 hours, while the simulation of the monolayer with an abnormal area takes 32.1 hours. For the continuum model, the simulation of the healthy

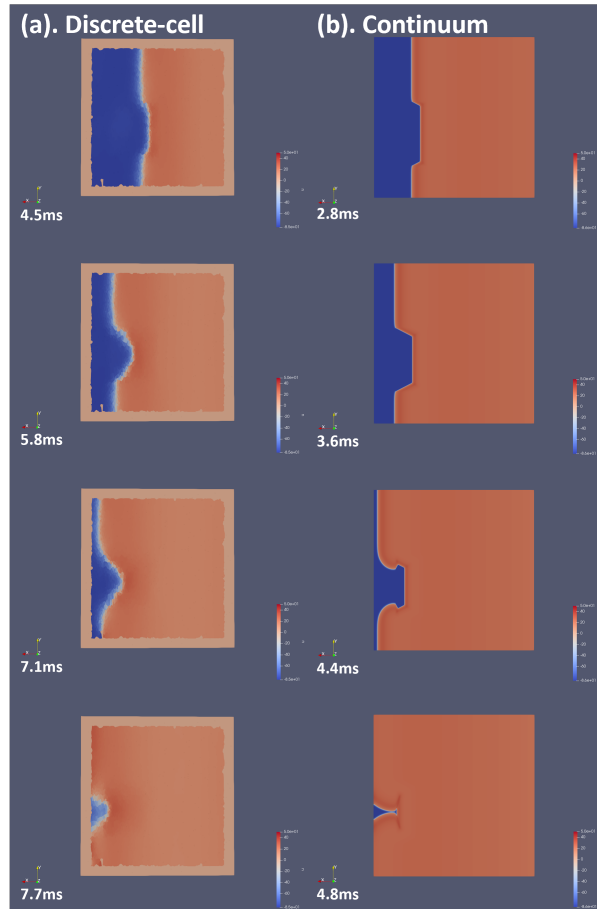


Figure 4. Simulated propagation within the abnormal area with (a) the discrete-cell model; (b) the continuum model.

monolayer takes 29 minutes, while the simulation of the abnormal monolayer takes 6.4 hours.

The EGM durations are significantly extended within the abnormal area for both models (mean 7.6 ms to 10.2 ms), shown in Figure 5(a). Additionally, EGM durations from the discrete-cell model have increase spread (standard deviation: 0.8471 in healthy area and 2.327 in abnormal area) compared to the continuum model (standard deviation: 0.037 in healthy area and 1.571 in abnormal area).

Figure 5(b) shows that the amplitudes of the EGMs are also affected by the abnormal area. The amplitudes of the EGMs from the abnormal area are reduced to the mean values of 0.194 mV for the discrete-cell model and 0.196 mV for the continuum model. The mean values from the healthy area are 0.376 mV and 0.378 mV respectively. The standard deviation of the amplitudes from the simulations with the continuum model (0.01 and 0.02) is also significantly smaller than those from the simulations with the discrete-cell model (0.05 and 0.045).

The impact of the abnormal area on the conduction ve-

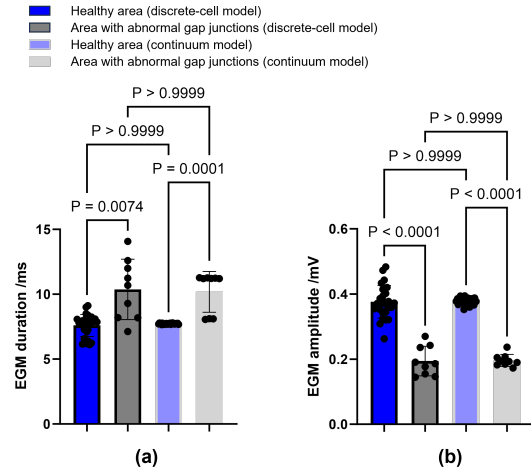


Figure 5. (a) Comparison of the durations of the EGMs. (b) Comparison of the amplitudes of the EGMs.

locity was analyzed (Figure 6). Despite visible slowing on the activation map (figure 4), the quantified difference between the conduction velocities within the healthy monolayer versus across both the healthy area and the abnormal area is not significant. However, all conduction velocities with the continuum model are higher than with the discrete-cell model. With the continuum model, the average conduction velocity of the propagation only in healthy area is 0.251 m/s and the velocity of the propagation going through both areas is 0.2131 m/s. With the discrete-cell model, the mean conduction velocities are 0.154 m/s and 0.134 m/s respectively.

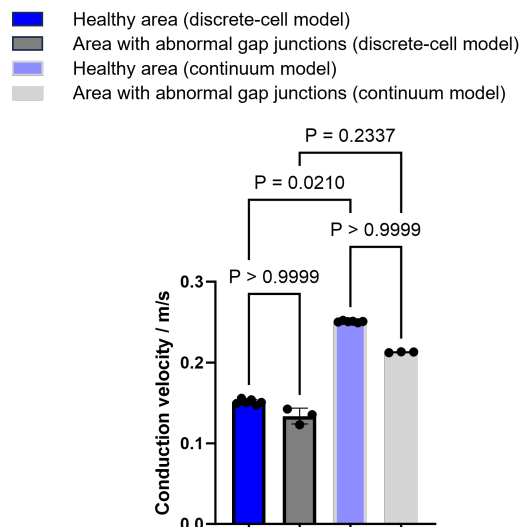


Figure 6. Comparison of the durations of the conduction velocities of the simulation with different models.

4. Discussion

This study examined how the type of propagation model influences the outputs from two-dimensional simulations of monolayers of human left ventricle myocytes. The results illustrate that both models provide similar time domain electrogram features with a $1.2 \text{ mm} \times 1.2 \text{ mm}$ simulation area. However, there was a difference in the conduction velocities between models. That may be due to increased detail from the presence of the gap junctions which are considered in the discrete-cell model, while the continuum model assumes the whole area is homogeneous. The gap junction resistance reduces the conduction velocities, therefore, the discrete-cell model may be more accurate than the continuum model at the cell-level simulation.

Although there was no significant difference in the mean values of time domain features, the spread of feature values in the discrete-cell model are much wider than those from the continuum model, likely due to the cell-level heterogeneity of the discrete-cell model. This suggests that the discrete-cell model may be more accurate at capturing cell level heterogeneity despite similar group comparisons.

The simulation time with the discrete-cell model is much longer than it is with the continuum model. If used to model a larger domain, this would be further increased, possibly rendering such simulations intractable without substantially larger computational resources[15, 16].

5. Conclusion

Even though the discrete-cell model requires much higher computational cost and time, these models more precisely capture biophysical processes and may provide more accurate simulated propagation results in the presence of heterogeneity of the monolayer. However, despite the assumptions within the continuum model, the feature outputs are comparable to the discrete cell model. While continuum models are essential for organ-scale simulation, discrete-cell models capture the propagation with greater biophysical accuracy and may provide a greater understanding of microscopic propagation within monolayers and myocardium.

References

- [1] Lippi G, Sanchis-Gomar F, Cervellin G. Global epidemiology of atrial fibrillation: An increasing epidemic and public health challenge. *International Journal of Stroke* 2021; 16:217–221.
- [2] Albert CM, Stevenson WG. The future of arrhythmias and electrophysiology. *Circulation* Jun. 2016;133:2687–2696.
- [3] Baldzizhar A, Manuylova E, Marchenko R, Kryvalap Y, Carey. MG. Ventricular tachycardias: Characteristics and management. *Critical Care Nursing Clinics of North America* 20016;28:317–329.
- [4] O’Hara T, Virág L, Varró A, Rudy Y. Simulation of the undiseased human cardiac ventricular action potential: Model formulation and experimental validation. *PLoS Computational Biology* 2011;7.
- [5] Moreau A, Gosselin-Badaroudine P, Chahine M. Biophysics, pathophysiology, and pharmacology of ion channel gating pores. *Frontiers in Pharmacology* Apr. 2014;5.
- [6] Peter C, Houston J. A multi-domain biophysical computational model of cardiac action potential propagation in cell monolayers. Ph.D. thesis, Imperial College London, 2021.
- [7] Kudryashova N, Tsvelaya V, Agladze K, Panfilov A. Virtual cardiac monolayers for electrical wave propagation. *Scientific Reports* 2017;7.
- [8] Dias P, Desplantez T, El-Harasis MA, Chowdhury RA, Ulrich ND, Diego ACD, Peters NS, Severs NJ, MacLeod KT, Dupont E. Characterisation of connexin expression and electrophysiological properties in stable clones of the h1-1 myocyte cell line. *PLoS ONE* 2014;9.
- [9] Geuzaine C, Remacle JF. Gmsh: A 3-d finite element mesh generator with built-in pre- and post-processing facilities. *International Journal for Numerical Methods in Engineering* Sep. 2009;79:1309–1331.
- [10] Peters NS, Coromilas J, Severs NJ, Wit AL. Disturbed connexin43 gap junction distribution correlates with the location of reentrant circuits in the epicardial border zone of healing canine infarcts that cause ventricular tachycardia. *Circulation* 1997;95:988–996.
- [11] Cantwell CD, Moxey D, Comerford A, Bolis A, Rocco G, Mengaldo G, Grazia DD, Yakovlev S, Lombard JE, Ekelschot D, Jordi B, Xu H, Mohamied Y, Eskilsson C, Nelson B, Vos P, Biotto C, Kirby RM, Sherwin SJ. Nektar++: An open-source spectral/hp element framework. *Computer Physics Communications* Jul. 2015;205–219.
- [12] Moxey D, Cantwell CD, Bao Y. Nektar++: Enhancing the capability and application of high-fidelity spectral/hp element methods. *Computer Physics Communications* 2020; 249:107–110.
- [13] Tusscher KHWJT, Noble D, Noble PJ, Panfilov AV, Tusscher T, Univ U. A model for human ventricular tissue. *Am J Physiol Heart Circ Physiol* 2004;286:1573–1589.
- [14] Letchumy MJ, Brook J, Ntagiantas K, Panagopoulos D, Agha-Jaffar D, Peters NS, Qureshi N, Chowdhury RA, Cantwell CD. The effects of electrode configuration on omnipolar electrograms: An in-silico approach. Technical report, Imperial College London, 2022.
- [15] Houston C, Tzortzis KN, Roney C, Saglietto A, Pitcher DS, Cantwell CD, Chowdhury RA, Ng FS, Peters NS, Dupont E. Characterisation of re-entrant circuit (or rotational activity) in vitro using the h11-6 myocyte cell line. *Journal of Molecular and Cellular Cardiology* 2018;119:155–164.
- [16] Handa BS, Roney CH, Houston C, Qureshi NA, Li X, Pitcher DS, Chowdhury RA, Lim PB, Dupont E, Niederer SA, Cantwell CD, Peters NS, Ng FS. Analytical approaches for myocardial fibrillation signals. *Computers in Biology and Medicine* 2018;102:315–326.